



Structure-based lead identification of ATP-competitive MK2 inhibitors

Tjeerd Barf, Allard Kaptein, Sander de Wilde, Ruud van der Heijden, Richard van Someren, Dennis Demont, Carsten Schultz-Fademrecht, Judith Versteegh, Mario van Zeeland, Nicole Seegers, Bert Kazemier, Bas van de Kar, Maaïke van Hoek, Jeroen de Roos, Henri Klop, Ruben Smeets, Claudia Hofstra, Jorrit Hornberg, Arthur Oubrie*

Merck Research Laboratories, MSD, PO Box 20, 5340 BH Oss, The Netherlands

ARTICLE INFO

Article history:

Received 11 February 2011

Revised 29 March 2011

Accepted 3 April 2011

Available online 16 April 2011

Keywords:

MAPKAPK2

MK2

Anti-TNF α

SBDD

Rheumatoid arthritis

ABSTRACT

MK2 kinase is a promising drug discovery target for the treatment of inflammatory diseases. Here, we describe the discovery of novel MK2 inhibitors using X-ray crystallography and structure-based drug design. The lead has in vivo efficacy in a short-term preclinical model.

© 2011 Elsevier Ltd. All rights reserved.

Inhibition of the action of the pro-inflammatory cytokines TNF α and IL-6 have shown both in animal models and in the clinic to be efficacious in the control of autoimmune diseases like rheumatoid arthritis or psoriasis. In addition to TNF α and IL-6 neutralization strategies via biologics, many pharmaceutical companies have worked on the development of p38 inhibitors in order to block the production of these pro-inflammatory cytokines. Although several p38 inhibitors have been tested in phase 2 clinical trials, none have progressed to phase 3 clinical trials.¹ The lack of progress seems due to two main findings. First, drug toxicity observed for p38 inhibitors tested in the clinic may result in dose-limiting efficacy. Secondly, p38 inhibition results in the activation of the ERK, JNK and IKK signaling pathways via a feedback control of TAK1.²

MAPK activated protein kinase 2 (MK2) is downstream from p38 in this pathway and a key mediator regulating the production of TNF α and IL-6. MK2 knockout mice show a strong reduction in disease incidence and disease severity score in the arthritic CIA model.³ Specific modulation of MK2 activity, without inhibition of other downstream signaling events is hypothesized to avoid p38-associated adverse events. In addition, MK2 does not participate in the feedback control of TAK1 and may therefore result in sustained inhibition of the inflammatory response mediated via the p38/MK2 signaling pathway.⁴ Furthermore, MK2 may be an interesting target for pharmacological modulation based on the

data for the MK2 heterozygote mice in the CIA model.³ Since the heterozygote mice also show a clear reduction in disease severity and in LPS-induced production of TNF α and IL-6,⁵ full inhibition of MK2 activity does not seem to be required to obtain a physiologically relevant effect.

In this letter, we report the discovery of a novel class of spiro- δ -lactam MK2 inhibitors using X-ray crystallography and structure based drug design. The project was instigated by determination of the X-ray structures of MK2 bound to two reference compounds, **1** and **2** (Figs. 1 and 2).⁶ This was done using a construct comprising residues 41–364,⁷ as was also described elsewhere.⁸

The X-ray structure of MK2:1 revealed hydrogen bonding interactions between (1) the compound's pyridine nitrogen and MK2 backbone NH of Leu141; (2) cyclic amide carbonyl and catalytic Lys93 (Fig. 2). The NH of the cyclic amide does not make a hydrogen bond with Asp207 as was observed in other structures of MK2:1.⁸ This is due to the presence of malonate in the active site, which was used as precipitant in the crystallization solutions.⁷ In our structure, the NH of the cyclic amide makes an artificial polar interaction with malonate rather than Asp207. The quinoline moiety of the inhibitor is located in the front pocket, which is open,

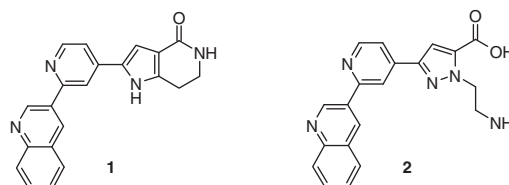


Figure 1. Pyrrolopyridinone **1** and pyrazole derivative **2**.

* Corresponding author.

E-mail address: arthur.oubrie@merck.com (A. Oubrie).

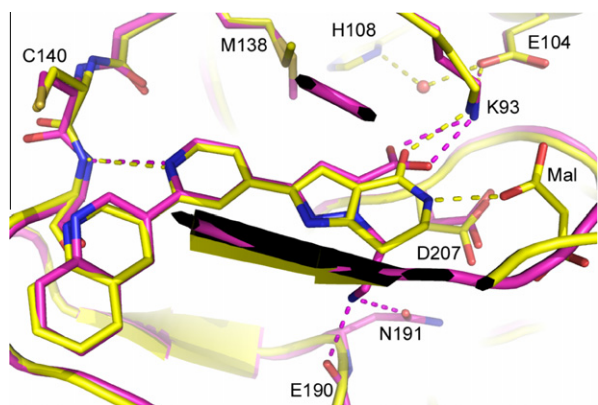


Figure 2. X-ray structures of MK2-41-364 bound to compounds **1** (yellow) and **2** (pink).⁷ Specific amino acids are labeled.

hydrophobic and has a flat surface, well suited to accommodate planar substitutions. The quinoline nitrogen is not involved in a hydrogen bond with protein or water, and the thiol of Cys140 is too far away for a direct interaction. However, the aryl ring stacks on top of the main chain carbonyl of Leu141, and a consistently short distance of ~ 3.2 Å was observed in all quinoline-containing structures. The structure of MK2:**2** showed that the quinoline and pyridine groups of the ligand make the same interactions with MK2 as in **1**. The carboxylic acid of **2** makes polar interactions with Lys93 and the main chain NH of Asp207, while the primary amine is hydrogen bonded to the carbonyl groups of the main chain of Glu190 and side chain of Asn191 (Fig. 2).

Analysis of these structures led to synthesis of a hybrid pyrazolopyridinone **3**, which combines the rigid lactam moiety of **1** with the primary amine of **2** (Fig. 3). A similar approach was followed by Pfizer researchers using the propylamine analogue of **2**, but in this

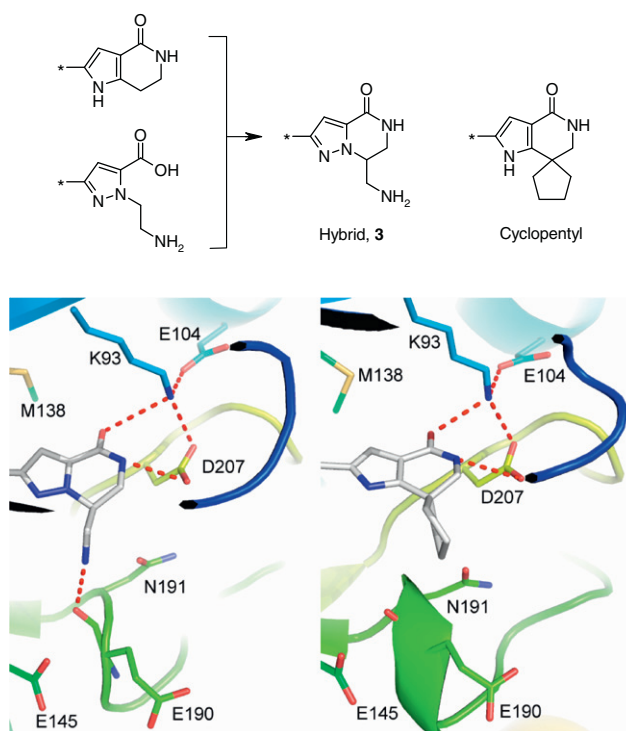


Figure 3. X-ray structures of MK2-41-264 complexed with pyrazole **3** and a cyclopentyl analogue.

case the methylamine group ends up alpha to the amide in the cyclized product.^{6a} In choosing the scaffold, the pyrazole was favored over the pyrrole owing to its greater synthetic accessibility, even though the pyrrole scaffold is normally superior to the pyrazole when comparing identical substructures. For instance, EC_{50} values of 8.5 and 216 nM were reported for pyrrole **1** and the otherwise identical pyrazole twin, respectively.^{6a} With an EC_{50} of 151 nM in our IMAP assay,⁹ hybrid compound **3** is not as potent as the reference compounds (EC_{50} -**1** = 49 nM; EC_{50} -**2** = 28 nM; Table 1), yet it demonstrated sufficient activity to be considered as a good starting point. In the ribose pocket, the crystal structure of MK2:**3** shows a similar binding mode to the previous protein:ligand structures with the cyclic amide forming a hydrogen bonding network with Lys93 and Asp207 (Fig. 3). The primary amine of **3** is hydrogen bonded to the main chain carbonyl of Glu190 but the distance to Asn191 appears too long for proper formation of a hydrogen bond. The position of the amine of **3** thus appears less optimal for the formation of polar interactions as compared to **2** and this may in part explain the relatively low inhibitory activity of **3**. Also, the reduced potency of **3** can be attributed to the absence of the ionic interaction as demonstrated in the MK2:**2** complex.

In the next step, we envisaged that incorporation of the amino function in a rigid aliphatic spiro ring would reduce the number of rotatable bonds and thus improve biochemical potency. However, the synthesis of those examples initially posed a challenge, since the optimal ring size and exact position of the basic amine was not known. To circumvent trial and error, we chose to examine the space in the ribose pocket first in terms of tolerability towards cycloalkyl rings in combination with the more potent pyrrolopyridinone scaffold. Another potential advantage of aliphatic ring systems was to overcome the lack of cellular activity observed for des-spiro derivative **3** (data not shown). Cyclopentyl analogues were the first derivatives we decided to explore owing to availability of starting materials and their relatively small size. A convergent synthesis route towards the cyclopentyl derivatives was employed (Scheme 1). For the generation of the key pyrimidine building block **C**, we relied on the Stille coupling reaction with an ethylvinyl tin reagent on 2,4-dichloropyrimidine. Direct bromination on the resulting enol ether **B** in ethanol was achieved to give **C** with high yield. Preparation of the cyclopentyl piperidinone started with acylation of commercially available 1-(aminomethyl)cyclopentane carboxylate **D** with ethyl malonyl chloride. Cyclization of **E** with a Dieckmann condensation and subsequent decarboxylation rendered intermediate **F** in good yields. Generally, the Paal–Knorr condensation reaction with chloropyrimidine derivative **C** worked reasonably well. The generation of final compound **4** was part of a small library effort, in which aryl moieties were introduced in varying yields on chloropyrimidine **G** via Suzuki coupling reactions. A number of analogues were prepared but no significant potency improvements were made within this chemical series (not shown).

Quinoline analogue **4** was among the most potent cyclopentyl pyrimidine MK2 inhibitors and exhibited a moderate biochemical potency (EC_{50} = 234 nM), comparable to methylamino derivative **3** (Table 1). A crystal structure of MK2 bound to a close analogue of **4** was introduced (Fig. 3). This structure indicated that the cyclopentyl ring fitted snugly in the ribose pocket, apparently located within hydrogen-bond distance of the main chain of Glu190 and side chain of Asn191. The cyclopentyl ring with its hydrophobic nature thus appears to be tolerated in the polar ribose pocket owing to the formation of weak polar interactions. Unfortunately, properties including compound polarity, membrane permeability, and microsomal stability varied significantly within this chemical series and optimization of all these parameters simultaneously appeared problematic. For instance, the kinetic solubility for this subseries was consistently low (Table 1). Introduction of polar aryl

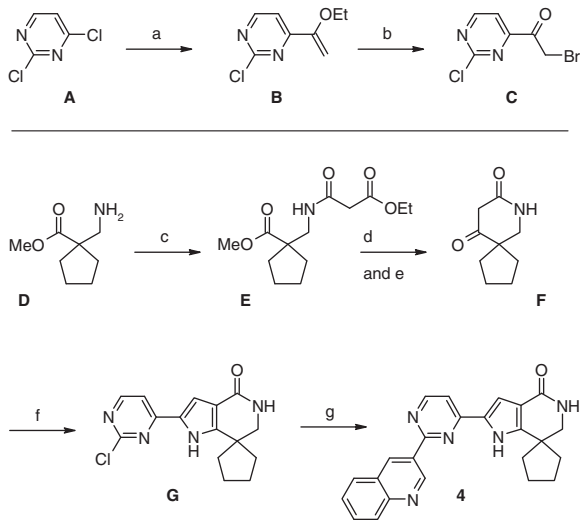
Table 1
Biochemical and cell activity, and in vitro ADME properties

Compound	MK2 IMAP EC ₅₀ ^a (nM)	TNF-THP1 EC ₅₀ ^b (μM)	PAMPA nm/s	Caco-2 nm/s	Kinetic solubility (pH 7.4, mg/L)	HLM/RLM (t _{1/2} min)	PPB (%)	c Log P
1	49	38%@10 μM	6	5	0	35/40	99.7	2.7
2	28	7%@10 μM	NT ^c	NT	33	NT/NT	NT	0.1
4	234	50%@10 μM	NT	NT	0	NT/NT	NT	3.5
5a	6	4.8	0	NT	23	NT/NT	NT	1.6
5b	4	0.98	0	1	37	91/>120	97.0	1.7

^a Values are means of two independent experiments with duplicates for each dilution per experiment.⁹

^b THP1 cells are pre-incubated for 30 min with MK2 inhibitors prior to stimulation with LPS. Values are means of duplicates for each dilution.¹⁴

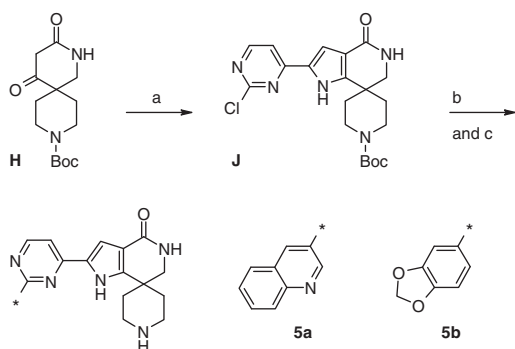
^c NT means Not tested.



Scheme 1. Reagents and conditions: (a) 1-Ethoxyvinyltri-*N*-butyltin, PdCl₂(Ph₃P)₂, DMF, 80 °C; KF workup (79%); (b) NBS, THF/H₂O (5/2), rt (89%); (c) ClCOCH₂COOEt, Et₃N, DCM, 0 °C–rt (72%); (d) NaOMe, MeOH, 65 °C; (e) ACN/H₂O (1/1), 80 °C (79%, two steps); (f) Cmpd. **C**, NH₄OAc, EtOH, rt (59%); (g) library: arylboronic acids, Pd(Ph₃P)₄, K₂CO₃, toluene/EtOH (4/1), 140 °C, MW (5–30%).

substitutions in the front pocket that were necessary to rescue solubility proved to be detrimental for membrane permeability, and thus cellular potency. Nevertheless, the cycloalkyl ring derivatives provided confidence that aza-spiro groups would be worthwhile pursuing, and this prompted us to investigate a third scaffold modification.

Compound **5a** and **5b** represent the combined effort (**Scheme 2**). The synthetic route towards these 4-piperidylpyridinone derivatives was largely identical to the preparation of cyclopentyl ana-



Scheme 2. Reagents and conditions: (a) Cmpd. **C**, NH₄OAc, EtOH, rt (29%); (b) arylboronic acid, Pd(Ph₃P)₄, K₂CO₃, toluene/EtOH (4/1), 140 °C, MW (c) 4 N HCl, dioxane, rt (33–44% in two steps).

logue **4**. The prerequisite Boc-protected oxolactam intermediate **H** was essentially prepared as described earlier,¹⁰ and in analogy with cyclopentyl oxolactam **F** as outlined in **Scheme 1**. After the Suzuki coupling with 3,4-methylenedioxyphenyl- or quinolin-3-ylboronic acid, the final envisaged products could be isolated following acidic removal of the Boc protective group.

The introduction of an amine function as in **5a** and **5b** resulted in improvement in terms of both potency and physicochemical parameters as compared to fully aliphatic rings (**Table 1**). Activity was improved to single digit nanomolar inhibition in biochemical assays for these, and for many other analogues.¹¹ Compound **5b** displayed the best overall profile since it inhibited LPS-induced TNF α production/release in THP1 cells (EC₅₀ = 0.98 μM) and peripheral blood mononuclear cells (PBMCs, EC₅₀ = 0.26 μM). The cellular inhibition was confirmed in the Hsp27 phosphorylation assay in THP1 cells (EC₅₀ = 0.62 μM), a target engagement marker for MK2 activity. Also, **5b** displayed a high degree of selectivity and kinases that are directly associated with the TNF α pathway were not inhibited at 1 μM.¹¹

The molecular basis for the MK2 inhibition is well understood on the basis of crystal structures of **5b** with both MK2 and MK3, a close analog of MK2. MK3 was recently described as a suitable surrogate structural model for MK2.¹² In our hands, crystals of MK3 could indeed be grown more readily than those of MK2. Furthermore, MK3 crystals contained only one rather than 12 molecules per asymmetric unit and diffracted to higher resolution.¹³

The structures of MK2 and MK3 bound to **5b** are shown in **Fig. 4**. The active sites of both proteins are indeed very similar, both in terms of amino acid composition and general architecture of the pocket. Only one amino acid is different, Leu141 (MK2) vs Met121 (MK3). This difference does not influence the shape, size, or physicochemical properties of the ATP pocket. Compound **5b** binds nearly identical to MK2 and MK3. In both structures and

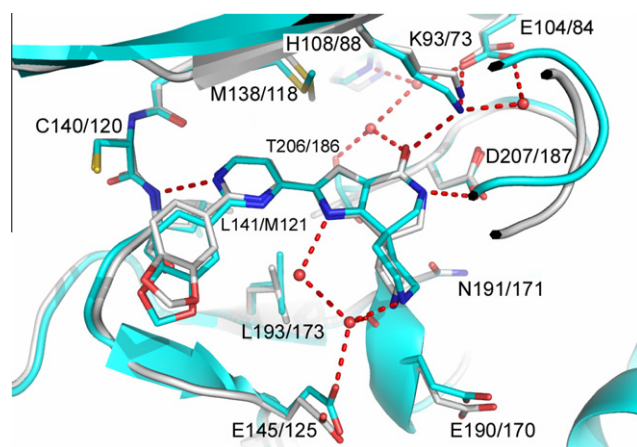


Figure 4. Crystal structures of **5b** in human MK2 (grey) and MK3 (cyan).¹² Specific amino acids are labeled.

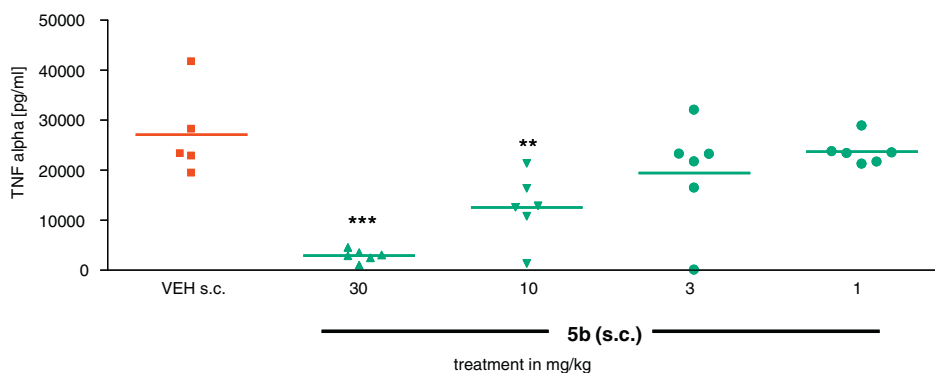


Figure 5. Dose response curve of LPS-induced release of TNF α in rats after subcutaneous dosing of **5b**.¹⁵ LPS was administered 1.5 h before extraction of blood. Statistically significant differences are indicated as **($p < 0.05$) and ***($p < 0.01$).

consistent with other MK2:inhibitor structures, one pyrimidine N forms a hydrogen bond with the main chain amide of Leu141/Met121 (MK2/MK3 numbering), and the cyclic amide of **5b** is in contact with Lys93/Lys73 and Asp207/187. In the structures, the basic amine is not involved in direct polar interactions with either Glu145 or Glu190, as was shown for **2**. The MK3:**5b** structure reveals an elaborate hydrogen-bonding network involving the pyrrole-NH, the basic amine, Glu145, and a number of water molecules. Due to the limited diffraction quality of MK2 crystals, such interactions could not be observed in our MK2 structures. However, on the basis of the otherwise high similarity between the MK2 and MK3 structures these interactions most likely also exist in MK2. In addition to this water-mediated hydrogen-bond network, the surface of both proteins is relatively acidic in the area of the ribose and phosphate sub-pockets. This suggests that part of the improvement in potency as a result of introducing a basic amine in our compounds can be attributed to the formation of beneficial electrostatic interactions.

In addition to improving potency, the introduction of a basic amine in **5b** also improved other properties including kinetic solubility, lipophilicity, plasma protein binding, and stability in human and rat liver microsomes (Table 1). On the other hand, absorption properties were compromised as a result of the presence of basic amines, see for example Caco-2 values (Table 1). This was also reflected by PK data in rats for **5** following per oral (p.o.), subcutaneous (s.c.) and intravenous (i.v.) dosing. The rat AUC was 0.016 $\mu\text{M h}$ after p.o. dosing at 10 $\mu\text{mol/kg}$, 1.26 $\mu\text{M h}$ after i.v. dosing at 4 $\mu\text{mol/kg}$, and 2.71 $\mu\text{M h}$ after s.c. dosing at 10 $\mu\text{mol/kg}$. These data showed that the compound does not get absorbed via the oral route, whereas availability is moderate following subcutaneous administration. Oral bioavailability thus became one of the main issues for this chemical series in lead optimization, which will be addressed in an accompanying paper.¹¹

The potential of **5b** to inhibit production of TNF α was analyzed in rats following s.c. and i.v. administration and an LPS challenge.¹⁵ Compound **5b** inhibited 85% and 92% of the TNF α release in rats following s.c. (30 mg/kg) and i.v. (12.5 mg/kg) administration, respectively. A dose response curve was also conducted after s.c. dosing. Fig. 5 shows a dose-dependent reduction of TNF α release with statistically significant inhibition at 10 and 30 mg/kg, of 54% and 89% respectively.

In conclusion, MK2 inhibitor **5b** was identified using structure-based drug design. The compound exhibits good potency in biochemical and in cell-based assays, including primary human cells (human PBMCs). It appeared clean in many toxicity assays and showed efficacy in short-term, preclinical in vivo models such as LPS-induced release of the cytokine TNF α . The major issue with

5b for further development was its lack of oral bioavailability and this will be addressed in an accompanying paper.

Acknowledgments

The authors wish to acknowledge Gerard Vogel for generating the PK data of **5b** and Joost Uitdehaag for stimulating discussions.

References and notes

- (a) Sweeney, S. E. *Nat. Rev. Rheumatol.* **2009**, *5*, 475–477; (b) Hammaker, D.; Firestein, G. S. *Ann. Rheum. Dis.* **2010**, *69*, 177.
- Cheung, P. C. F.; Campbell, D. G.; Nebreda, A. R.; Cohen, P. *EMBO J.* **2003**, *22*, 5793.
- Hegen, M.; Gaestel, M.; Nickerson-Nutter, C. L.; Lin, L.-L.; Telliez, J.-B. *J. Immunol.* **2006**, *177*, 1913.
- Ronkina, N.; Menon, M. B.; Schwermann, J.; Tiedje, C.; Hitti, E.; Kotlyarov, A.; Gaestel, M. *Biochem. Pharmacol.* **2010**, *80*, 1915.
- Kotlyarov, A.; Neiningner, A.; Schubert, C.; Eckert, R.; Birchmeier, C.; Volk, H. D.; Gaestel, M. *Nat. Cell. Biol.* **1999**, *1*, 94.
- (a) Hanau, C. E. et al. WO patent 2004058176; (b) Anderson, D. R. et al. WO patent 2004058762; (c) Anderson, D. R.; Meyers, M. J.; Vernier, W. F.; Mahoney, M. W.; Kurumbail, R. G.; Caspers, N.; Poda, G. I.; Schindler, J. F.; Reitz, D. B.; Mourey, R. J. *J. Med. Chem.* **2007**, *50*, 2647.
- Structures of MK2:**1** and MK2:**2** were determined in collaboration with Sareum and obtained using a construct comprising residues 41–364 with a C-terminal His-tag. This construct was expressed in *Escherichia coli* and purified using immobilized metal affinity, size exclusion, and ion exchange chromatography. The protein was crystallized in space group P 4₃2 using malonate as precipitant. Data sets with **1** and **2** were collected at 3.0 and 3.2 Å, respectively. The coordinates have been deposited with the Protein Data Bank at Rutgers, the respective codes are 3R2Y and 3R3O.
- (a) Underwood, K. W.; Parris, K. D.; Federico, E.; Mosyak, L.; Czerwinski, R. M.; Shane, T.; Taylor, M.; Svenson, K.; Liu, Y.; Hsiao, C. L.; Wolfrom, S.; Maguire, M.; Malakian, K.; Telliez, J. B.; Lin, L. L.; Kriz, R. W.; Seehra, J.; Somers, W. S.; Stahl, M. L. *Structure* **2003**, *11*, 627; (b) Hillig, R. C.; Eberspaecher, U.; Monteclaro, F.; Huber, M.; Nguyen, D.; Mengel, A.; Muller-Tiemann, B.; Egner, U. *J. Mol. Biol.* **2007**, *369*, 735.
- MK2 enzyme activity is measured using an IMAP assay (Immobilized Metal Assay for Phosphochemicals-based coupled assay). Test compounds in DMSO (final concentration is assay is 0.1% DMSO) and MK2 enzyme (peptide 46-end (Millipore) 25 mU/mL final concentration in assay) are pre-incubated 30 min at room temperature, before adding Fluorescein labeled substrate peptide (Fluo-betaA-11A NeoMPS, final substrate peptide concentration is 50 nM). Kinase assay is started by adding ATP (final ATP concentration is 1 μM (=K_m ATP)). Following incubation for 2 h at room temperature the enzyme reaction is stopped by adding IMAP Progressive Binding Solution (according to suppliers (Molecular Devices) protocol). After 60 min incubation at room temperature in the dark the FP signal is read. Each concentration is tested in two independent experiments with duplicates in each experiment.
- Revesz, L.; Schlapbach, A.; Aichholz, R.; Dawson, J.; Feifel, R.; Hawtin, S.; Littlewood-Evans, A.; Koch, G.; Kroemer, M.; Möbitz, H.; Scheufler, C.; Velcicky, J.; Huppertz, C. *Bioorg. Med. Chem. Lett.* **2011**, *20*, 4719.
- Kaptein, A.; Oubrie, A.; Zwart, E. de; Hoogenboom, N.; Wit, J. de; Kar, B. van de; Hoek, M. van; Vogel, G.; Kimpfe, V. de; Schultz-Fademrecht, C.; Borsboom, J.; Zeeland, M. van; Versteegh, J.; Kazemier, B.; Roos, J. de; Wijnands, F.; Dulos, J.; Jaeger, M.; Leandro-Garcia, P.; Barf, T. *Bioorg. Med. Chem. Lett.* **2011**. doi:10.1016/j.bmcl.2011.04.016.
- Cheng, R.; Felicetti, B.; Palan, S.; Toogood-Johnson, I.; Scheich, C.; Barker, J.; Whittaker, M.; Hestekamp, T. *Protein Sci.* **2010**, *19*, 168.

13. In house structures of MK2 and MK3 bound to **5b**: The MK2 structure was obtained using a construct comprising residues 41-364 with a cleavable N-terminal His-tag. MK2 protein was purified using immobilized metal affinity, size exclusion, ion exchange chromatography and removal of the His-tag with Thrombin. This construct crystallized in space group $P 2_12_12_1$ with 12 molecules per asymmetric unit. The structure of MK2:**5b** was determined at 2.9 Å resolution. MK3 protein was purchased from Evotec and crystallized with **1** using protocols described in Ref. 12. MK3:**1** crystals were soaked and exchanged with **5b**. The structure of MK3:**5b** was determined at 2.1 Å resolution. The coordinates have been deposited with the Rutgers Protein Data Bank, with accession codes 3R2B and 3R1N.
14. THP1 cells are seeded at 1.5×10^5 cells per well in DMEM F12 (Gibco) supplemented with Penicilin/Streptomycin (80 U/mL; 80 µg/mL) and 10% FBS (Fetal Bovine Serum) in 96 well plate. Cells are left to rest for at least 18 h in a humidified atmosphere at 5–7% CO₂ at 37 °C, prior to incubation with test compounds. Dilutions of test compounds in DMSO (0.1% DMSO final concentration in assay) are added to the cells. Following a 30 min incubation LPS is added (final LPS concentration 10 µg/mL). Following a 4 h incubation at 5–7% CO₂ at 37 °C in humidified atmosphere, culture medium is collected for the measurement of TNFα. The amount of TNFα in the culture medium is quantified by ELISA using HuTNFα assay from Cytoset according to protocol.
15. Rats are treated with different compound doses. Control animals are treated with placebo. 1 h after compound treatment, rats are intraperitoneally injected with LPS (0.5 mg/kg). 1.5 h after LPS injection, serum is collected for the measurement of TNFα level. The amount of TNFα in the serum is quantified by ELISA.